An OpenFOAM Solver for Shock and Detonation Simulation in Real Gas

Zifeng Weng, Rémy Mével
Center for Combustion Energy, School of Vehicle and Mobility, State Key Laboratory for
Automotive Safety and Energy, Tsinghua University 30 Shuang Qing road, Beijing, China

1   Introduction

In order to achieve higher fuel storage and consumption efficiency in energy systems, high-pressure conditions are widely used in renewable energy storage strategies, and in conventional fossil fuel utilization. At high pressure, the interactions between molecules as well as their finite volume, neglected by the ideal gas (IG) assumption, becomes significant. Out of the purpose of safety evaluation, it is worthy understanding the shock and detonation dynamics in relevant devices. The shock compression will further increase pressure which makes the consideration of these real gas (RG) behaviors more important. It has been shown that the detonation speed [1], reaction zone structure [2, 3] and regularity of cellular structures [4] are significantly affected by the RG effects and cannot be captured by IG model.

Several simulation tools capable of describing real gas have been developed, RAPTOR [5, 6], AVBP [7], CharlesX [8]. They have been mainly used for numerical studies of transcritical or supercritical injection, droplet vaporization, mixing, and combustion in liquid rocket engine, which has been reviewed recently by Bellan [9]. However, these tools are not open source. Recently, efforts have been devoted to implement RG model in open source platform OpenFOAM. Traxinger et al. [10] have implemented a pressure-based solver for sub- and super-sonic flows considering RG effects and phase separation. Shahsavari et al. developed a large-eddy simulation (LES) solver [11]. Nguyen et al. [12] noted that the mixing rule in OpenFOAM is not suitable for RG. They developed a real-fluid thermophysical library in OpenFOAM which can be directly coupled with solvers in OpenFOAM. However, RG based numerical solver for shock and detonation appears to be a rarely explored topic. This work thus seeks to develop an OpenFOAM solver for unsteady, multi-dimensional, shock and detonation simulation in real gas. The new solver is referred to as Real gas Shock and Detonation OpenFAOM solver (RSDFoam).

2   Governing Equations and Numerical Methods

The viscosity and diffusion were neglected, as usually done for shock and detonation simulation [4]. The governing equations thus correspond to the non-reactive or reactive Euler equations, which read

$$\frac{\partial}{\partial t}\begin{pmatrix}\rho \\ \rho Y_i \\ \rho \mathbf{u} \\ \rho E\end{pmatrix} + \nabla \cdot \begin{pmatrix}\rho \mathbf{u} \\ \rho Y_i \mathbf{u} \\ \rho \mathbf{u} \otimes \mathbf{u} + P\mathbf{I} \\ (\rho E + P)\mathbf{u}\end{pmatrix} = \begin{pmatrix}0 \\ \dot{R}_i \\ 0 \\ 0\end{pmatrix}, \tag{1}$$

where ρ is density, $\mathbf{u}$ is the velocity vector, Y_i is the mass fraction of the ith species, $\dot{R}_i$ is the rate of production of the ith species, P is pressure, E is the total energy, i.e., the sum of internal energy (e) and

kinetic energy ($\mathbf{u} \cdot \mathbf{u}/2$), $\mathbf{I}$ is the unit tensor. The rate of production of the ith species is calculated with

$$\dot{R}_i = W_i \sum_j (v_{i,j}^{''} - v_{i,j}^{'})\dot{r}_j, \tag{2}$$

where W_i is the molecular weight of the ith species, $v_{i,j}^{''}$ and $v_{i,j}^{'}$ are respectively the stoichiometric coefficients as product and as reactant of the ith species in the jth reaction, and $\dot{r}_j$ is the net reaction rate of the jth reaction. Two equations of state (EoS) for real gas were implemented, i.e., the Redlich Kwong (RK) EoS, and the Noble-Abel (NA) EoS. According to the work of Schmitt et al. [3], the RK EoS has a good trade-off between accuracy and complexity among various cubic EoS. It reads

$$P = \frac{\rho R T}{1 - \rho b} - \frac{a \rho^2}{1 + \rho b}, \tag{3}$$

where R is the universal gas constant (R_u) divided by the mean molecular weight; a and b are mass specific parameters to account for the inter-molecular attraction forces and the finite volume of molecules or atoms respectively. The parameters a and b are related to the critical properties (T_c, P_c) as

$$a = 0.42748 \frac{R^2 T_c^{2.5}}{P_c T^{0.5}}, \; b = 0.08664 \frac{R T_c}{P_c} \tag{4}$$

At high temperature and pressure conditions, the inter-molecular attraction might be less important and could be neglected under certain conditions by setting $a = 0$ [4], leading to the NA EoS. In this case, b is obtained using $b = R T_c/8 P_c$, or fitted to experimental data. For the RG EoS, each thermodynamic function consists of an ideal part and the departure function, which is specific to the EoS considered. Details can be found in [2, 3]. The mass action law for RG was derived by Giovangigli et al. [13]

$$\dot{r}_j = k_{f,j} \prod_i \left(\phi_i \frac{X_i P}{RT} \right)^{v_{i,j}^{'}} - k_{r,j} \prod_i \left(\phi_i \frac{X_i P}{RT} \right)^{v_{i,j}^{''}}, \tag{5}$$

where X_i and ϕ_i are the mole fraction and fugacity coefficient of the ith species; $k_{f,j}$ and $k_{r,j}$ are the forward and backward reaction rate constant of the jth reaction. The reaction rate $k_{f,j}$ is in Arrhenius form, while $k_{r,j}$ equals to $k_{f,j}/K_{c,j}$ where $K_{c,j}$ is the equilibrium constant. Details can be found in [2].

RSDFoam was developed in OpenFOAM 9 by connecting blastFoam v5.0 [14] and Cantera v2.4 [15]. The convection and reaction source terms of reactive Euler equations are handled separately using operator splitting and explicit, semi-discrete approaches. The first step neglects the reaction source while the second step takes the chemical reaction into account using a constant volume reactor model. The latter is fulfilled using 0D solvers in Cantera. The numerical schemes, including high-order time integration, reconstruction and flux evaluation, were provided by blastFoam. To ensure simulation can be performed with a high-enough resolution while maintaining a reasonable computational cost, 1D to 3D adaptive mesh refinement (AMR) was included in the solver. The real gas models are handled in Cantera, in which non-ideal EoS, thermodynamic functions and reaction kinetic law were implemented.

3   Validation for Non-reactive Simulation

3.1   Sod shock tube problem

Figure 1 presents the solutions for the Sod shock tube problem obtained analytically and numerically. Both IG and RG are considered. At initial state, the pressure ratio P_5/P_1 is 20, the temperature ratio

T_5/T_1 is 1 and γ^0 is fixed at 1.4. Subscript 5 refers to the driver section. It is noted that at the same temperature and pressure, the values of a and b depends on the specific species considered. Out of generality, non-dimensional parameters, i.e., $A = aP/R^2T^2$, $B = bP/RT$, are used and it is assumed that $A = B = 0.1$ in the driver section, which corresponds to $T_1 = 448.0$ K and $P_1 = 16.9$ MPa for oxygen, $T_1 = 552.3$ K and $P_1 = 15.4$ MPa for methane, etc. Since the EoS is changed from IG to RK, the density calculation is changed. Figure 1 shows that RK EoS leads to much smaller density ratio ρ_5/ρ_1. However, the speed of the shock wave seems slightly affected by the RG model. The relative difference is only 2.1%. The strength of the shock wave is weaker for RG as seen from the smaller amplitude of the shock jump. Quantitatively, the Mach number for IG and RG cases are 1.83 and 1.76. Also, the RG model leads to a wider expansion fan and a lower propagation speed of contact surface. The numerical results were found to agree well with analytical solutions, both for IG and RG case.

(a) P   (b) T   (c) ρ
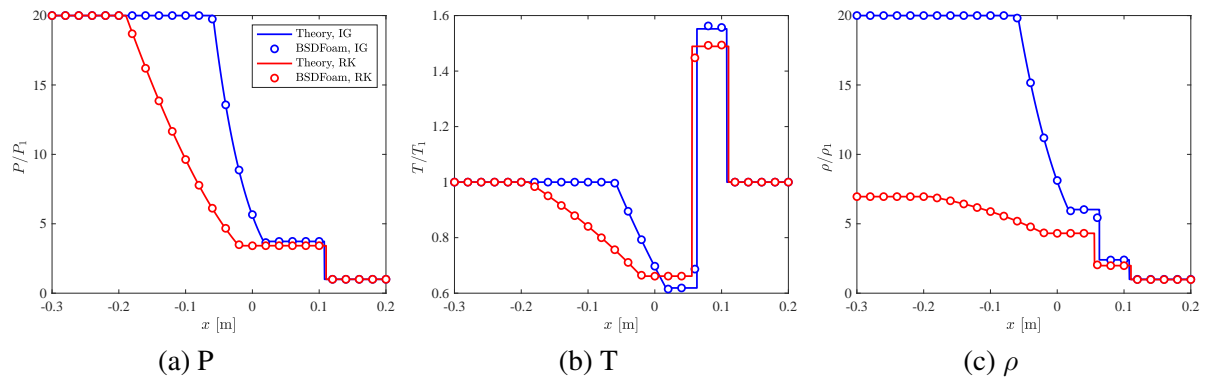
Figure 1: Analytical and numerical solutions of Sod shock tube problem at $t = 0.05$ s. Both IG and RG ($A = B = 0.1$ in driver section) are considered. (a) pressure, (b) temperature, (c) density.
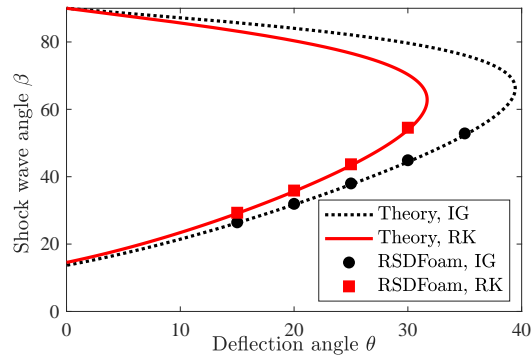
Figure 2: Oblique shock wave angle and deflection angle relation calculated for IG gas and RK gas. $u_1/U_{ref} = 5$. $\gamma^0 = 1.4$. $A = B = 0.1$.

3.2   Oblique shock

To validate RSDFoam, two-dimensional simulation of the interaction of a supersonic flow with a wedge were performed using a 0.5×0.5 m^2 domain. The base mesh is 0.01×0.01 m^2 with 4 levels of mesh refinement. The shock polar, i.e., the relation between the shock (β) and deflection (θ) angles, obtained analytically and numerically are compared in Fig. 2 for several conditions. The inflow speed is fixed as $u_1/\sqrt{RT_1} = 5$. γ^0 is 1.4 while A and B are both 0.1. It is found that the shapes of the shock polars are similar for IG and RK EoS, i.e., a backward 'C' shape. In either case, the polar has a unique maximum

deflection angle θ_{max}. If $\theta < \theta_{max}$, there are two possible values of β for each θ. The larger one corresponds to the strong shock solution while the smaller one corresponds to the weak shock solution. When using RK EoS, it is found that a smaller θ_{max} is obtained. In addition, the strong shock solution becomes lower while the weak shock solution becomes larger compared to the results for IG. In the numerical simulation, only the weak shock solution is obtained for both IG and RK EoS. The results, denoted with symbols in Fig. 2, are close to the analytical solutions. The results convincingly indicate that RSDFoam along with 2D AMR are capable of simulating 2D inert shock dynamics.

4 Validation for Reactive Simulation

4.1 Detonation speed

To evaluate the performance of RSDFoam for detonation simulation, we verified if the solver can give accurate detonation speed, which is an essential parameter for detonation simulation. The steady detonation speed is well described by the Chapman-Jouguet (CJ) theory which was solved using an in-house solver developed on Cantera [2]. In addition, 1D unsteady simulations were carried out for a stoichiometric H_2-air mixture. The detonation speeds obtained with the CJ theory and RSDFoam are presented in Fig. 3 along with the experimental data from Bauer et al. [1]. The CJ speed obtained with RK EoS is higher than the one calculated with the IG EoS. The difference is observed starting from approximately 1 MPa and increases with the initial pressure. Moreover, the CJ speed of RK gas is in better agreement with the experimental data. By performing 1D unsteady simulation using RSDFoam, the detonation speed was close to the CJ speed. The second column of Fig. 3 presents the relative difference between the CJ speed and the results from RSDFoam. The difference is less than 0.1% when using the IG EoS, while it reaches a maximum of 0.6% when using the RK EoS. This is reasonable given the difference of assumptions made to obtain the equilibrium CJ velocity and the velocity from the unsteady simulations.
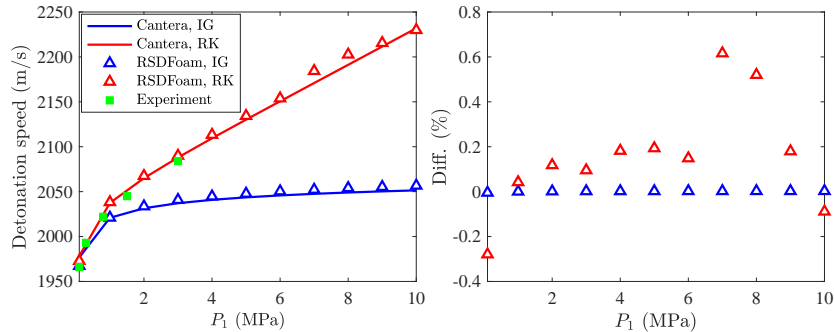
Figure 3: Comparison of steady detonation speed calculated with CJ theory and RSDFoam, and measured by Bauer et al. [1]. The fresh mixture is stoichiometric H_2-air initially at 300 K and 0.1-10 MPa.

4.2 Cellular structure simulation

To demonstrate the capability of the RSDFoam solver for unsteady and multi-dimensional detonation simulation, we simulated the cellular detonation following the pioneering work done by Taileb et al. [4]. They assumed a one-step irreversible reaction, of the form $\mathcal{R} \rightarrow \mathcal{P}$, so that the reaction rate is given by

$$\dot{R}_1 = -\rho A_s y_{\mathcal{R}} \exp\left(-\frac{E_a}{R_u T}\right), \tag{6}$$

where A_s is the pre-exponential factor, E_a is the activation energy, $y_{\mathcal{R}}$ is the mass fraction of reactant. E_a is $20R_uT_1$; A_s was 1.25×10^9 mol/m^3/s for IG EoS and was 1.10×10^9 mol/m^3/s for NA EoS; the amount of heat released was $q = 50R_uT_1$. The initial temperature and pressure were 300 K and 5 MPa. The heat capacity ratio was fixed at 1.2. The NA EoS was used with $b = 9.38 \times 10^{-4}$ m^3/kg. The grid size was $l_{1/2} \times l_{1/2}$ and 4 levels of AMR were applied to resolve the detonation front. The size of the domain was $150l_{1/2}$ in width and $1500l_{1/2}$ in length. $l_{1/2}$ is the half reaction length.

Figure 4 presents the numerical soot foil obtained with RSDFoam. After initiation, large detonation cells are recorded between $0 < x/l_{1/2} < 150$. Starting from approximately $200l_{1/2}$, the number of cell increases and their mean size decreases. As $x/l_{1/2} > 750$, the detonation reaches the self-sustained regime. For the NA gas, a regular cellular structure is formed, while when for the IG, the cellular structure is significantly more irregular. Such results are consistent with the findings of Taileb et al. [4], who attributed such a behavior to the increase of the isentropic coefficient induced by the finite molecular volume. With larger isentropic coefficient, the shock front bifurcation and formation of new triple point and associated sub-structure take place less frequently and thus the cellular structure is more regular.
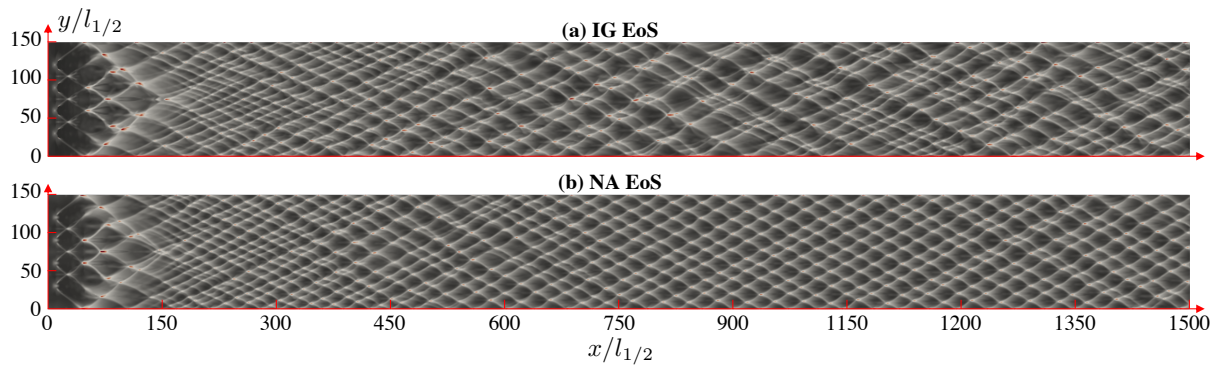
Figure 4: Numerical soot foils obtained with (a) IG EoS and (b) NA EoS. $P_1 = 5$ MPa and $P_1 = 300$ K.

To make a quantitative comparison, the cell width (λ) was measured manually in the range $1000l_{1/2} < x < 1500l_{1/2}$, which contains approximately 180 samples. The probability density function of the cell width is presented in Fig. 5. The cell width obtained with the IG EoS has a wider distribution than the one obtained with the NA EoS. The ranges of cell width are $6l_{1/2}$ to $32l_{1/2}$ and $10l_{1/2}$ to $27l_{1/2}$ when using the IG and NA EoS, respectively. These two ranges are close to those reported by Taileb et al. [4]: $9l_{1/2}$ to $37l_{1/2}$ for IG EoS and $7l_{1/2}$ to $35l_{1/2}$ for NA EoS. Despite the difference in cell regularity, Taileb et al. [4] found that the average cell widths for the two EoS are close, i.e., around $20l_{1/2}$. This finding was also confirmed in the present simulation. The average cell widths are $18.3l_{1/2}$ for IG and $20.2l_{1/2}$ for NA gas. The difference between the two works may be attributed to the different numerical schemes implemented in the two solver. Taileb et al. uses a ninth-order monotonicity preserving scheme for reconstruction of characteristic variables while RSDFoam uses MUSLC method which has a lower order of accuracy. In addition, uniform mesh was used in their work instead of using a coarse mesh along with AMR. Considering these differences, the agreement between the two solvers is satisfactory.

5   Conclusion

An OpenFOAM solver for shock and detonation simulation in real gas was developed by connecting blastFoam and Cantera. The connection enables using multiple numerical approaches from blastFoam and utilizing efficient chemistry model and real gas model from Cantera. The new solver, RSDFoam, has been validated with four test cases in the present work, including (1) Sod shock tube problem,
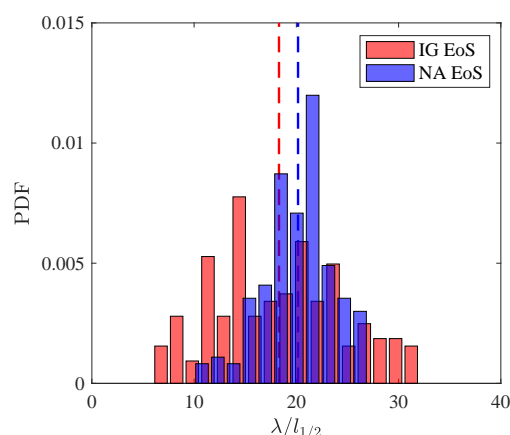
Figure 5: Probability density function of cell width for IG and NA EoS. The cell width was measured in the range of $x > 1000l_{1/2}$. Dashed lines denote the average values of cell width.

(2) oblique shock, (3) steady detonation speed, (4) cellular detonation. Satisfactory agreements were achieved for all the cases when comparing the simulation results with analytical solutions, previous simulation results or experimental data. RSDFoam will be a useful tool to improve our understanding on shock and detonation behaviors in non-ideal fluid.

References

[1] Bauer PA. (1985). Ph.D. Université de Poitiers.

[2] Weng ZF, Mevel R. (2022). Combust. Flame. 245: 112318.

[3] Schmitt RG. (1994). Ph.D. The University of Iowa, Iowa, United States.

[4] Taileb S, Melguizo-Gavilanes J, Chinnayya A. (2021). Phys. Fluid. 33: 036105.

[5] Oefelein JC, Yang V. (1998). J. Propul. Power. 14(5): 843.

[6] Oefelein JC. (2005). Proc. Combust. Inst. 30(2): 2929.

[7] Schmitt T, Selle L, Ruiz A, Cuenot B. (2010). AIAA Journal. 48(9): 2133.

[8] Ma PC, Lv Y, Ihme M. (2017). J. Comput. Phys. 340: 330.

[9] Bellan J. (2020). Combust. Sci. Technol. 192(7): 1199.

[10] Traxinger C, Zips J, Banholzer M, Pfitzner M. (2020). Comput. Fluids. 202: 104452.

[11] Shahsavari M, Wang B, Zhang B, Jiang G, Zhao D. (2021). J. Fluid Mech. 915: A47.

[12] Nguyen DN, Jung KS, Shim JW, Yoo CS. (2022). Comput. Phys. Commun. 273: 108264.

[13] Giovangigli V, Matuszewski L, Dupoirieux F. (2011). Combust. Theory Modell. 15: 141.

[14] Heylmun J, Vonk P, Brewer T. (2019). Synthetik Applied Technologies, LLC.

[15] Goodwin DG, Moffat HK, Schoegl I, Speth RL, Weber BW. (2018). https://www.cantera.org.